



Adsorption of Triton X-100 in aqueous solution on activated carbon obtained from waste tires for wastewater decontamination

Aida Mireya Ramírez-Arias¹ · Juan Carlos Moreno-Piraján¹ · Liliana Giraldo²

Received: 30 January 2019 / Revised: 20 July 2019 / Accepted: 23 July 2019 / Published online: 6 August 2019
© Springer Science+Business Media, LLC, part of Springer Nature 2019

Abstract

Adsorption of Triton X-100 non-ionic surfactant in aqueous solution on activated carbon was performed. The activated carbon was prepared from waste tires by chemical impregnation at 10, 20, 30, and 40% w-w⁻¹ of potassium hydroxide. Two carbonization temperatures, 700 and 900 °C were used with a heating rate of 2 °C·min⁻¹ and a 3 h retention time in N₂ flow of 100 mL·min⁻¹. The carbons obtained were characterized by N₂ adsorption at -196 °C, scanning electron microscopy, infrared microscopy, thermogravimetric analysis, and titration of functional groups. In adsorption studies of Triton X-100, the amount of adsorbed Triton X-100 was characterized by High-performance Liquid Chromatography and Langmuir, Freundlich, Toth, and Redlich-Peterson models were evaluated. The solids showed an area between 42 and 528 m²·g⁻¹ with characteristic isotherms of micro-mesoporous solids, and a pore distribution of 7.0 to 8.0 Å by Dubinin-Astakov with a chemical surface having acid and basic groups. The carbon that adsorbed the most Triton X-100 was QK409 with Q₀ 220 mg·g⁻¹.

Keywords Adsorption · Activated carbon · Surfactant · Waste tire · Waste water · Triton X-100

1 Introduction

Water pollution caused by surfactants has been increasing in recent years due to the great use of these in domestic life, agriculture, and industry. Surfactants or surface-active agents are amphiphilic organic compounds, which means that they are composed of a polar part (hydrophilic) and a non-polar part (hydrophobic). The surfactants have a characteristic head and tail in their chemical structure. In the head is the hydrophilic part, which defines the type of surfactant, and the hydrophobic in the tail (Zeng et al. 2007; Rosen 2004). These have unique properties that reduce surface tension and therefore are widely used as detergents, emulsifiers, foamers, and solubilizers (Lin et al. 1998). According to their chemical structure, surfactants are defined by the part known as the head which can be ionic, cationic, anionic or

nonionic (Zeng et al. 2007). Cationic surfactants due to their positive charge can be toxic (Jiménez et al. 2001). In general, ionic surfactants are more toxic than non-ionic surfactants, but there are exceptions. For example, linear alkylbenzene sulfonate is biodegradable and non-toxic (Zeng et al. 2007). Triton X-100 is among the non-ionic surfactants that are widely used as a solubilizing agent.

Triton X-100 is a non-ionic surfactant produced from octylphenol polymerized with X-ethylene oxide (Robson and Dennis 1997), with approximately n = 9.5 units of ethylene oxide by molecule, as illustrated in Fig. 1. This is formed by a hydrophilic part of polyethylene oxide and a hydrophobic part of aromatic hydrocarbon.

Triton X-100 is commonly used in molecular biology to isolate membrane protein complexes (Johnson 2013), in histology and microscopy laboratories like a wetting agent (Koley and Bard 2010), as well as electronic industry (Datta et al. 1997), and in polymer chemistry as an emulsifier and stabilizer (Fazley et al. 2017). In addition, it also has a global use as a cleaning product, such as a component in the manufacture of coated paints (Zeppieri et al. 2009) and as a surfactant in the biodegradation of petroleum hydrocarbons (Minoui and Minai 2009). According to Technavio analysts, the global market of Triton X-100 at a compound annual growth rate (CAGR) is near to 5%, where its growth

✉ Juan Carlos Moreno-Piraján
jumoreno@uniandes.edu.co

¹ Departamento de Química, Facultad de Ciencias, Universidad de los Andes, Cra. 1 #18a-12, Bogotá, Colombia

² Departamento de Química, Facultad de Ciencias, Universidad Nacional de Colombia, Cra 45, Bogotá, Colombia

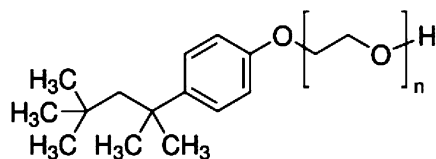


Fig. 1 Chemical structure of the Triton X-100 (TX-100)

in the market is driven by improving the biodegradation of oil hydrocarbons (Technavio 2018).

In addition, Triton X-100 is also used in various areas of everyday life, where waste is discharged into the drains. These residues end up in the water sources causing pollution of rivers and oceans, it affecting directly the water resources. Consequently, the water supplies for human consumption (Dinesh 2018).

Latin America has the privilege of being one of the regions with the greatest water resources in the world, harboring a third of the planet's water; each inhabitant has 60 m³ per day and additionally they have 28% of land with potential availability to be used in agriculture. However, there are few adequate institutional guidelines to manage water resources, which is why it is necessary to implement policies that ensure a satisfactory use of these resources to ensure that productivity increases and that the entire population has water services (Mejía et al. 2012). Appropriate water management implies control, mitigation of floods, droughts, and control of water pollution. In recent years, pollution has generated, increasingly recurrent catastrophic droughts and floods with negative impacts on human beings, either by the consumption of contaminated water or by dehydration. Several types of systems have been synthesized that have allowed cities to address this type of contamination in order to reduce it and/or to control it. Other materials commonly used are clays, pillared clays, zeolites, ceramic foams, carbon foams, and activated carbon. In the case of Triton X-100, several ways to treat this pollutant have been found. Two of these processes are biodegradation and adsorption. In the case of biodegradation, studies reported the use of yeast extract in the presence of active pollutants such as naphthalene and hexadecane, and showed that Triton X-100 is biodegradable in anaerobic and aerobic conditions depending on the type of organism and its concentration (Abd-allah and Srorr 1998; Mohan et al. 2006). Other studies have found Triton X-100 in sludge in the anaerobic digestion of lactose in the treatment of waste water (Parra 2015). With regard to adsorption, it has been studied adsorption of Triton X-100 in polystyrene particles (Romero et al. 2000), and adsorption of Triton X-100 in carbon paste (Niranjana et al. 2007).

Specifically in adsorption, porous solids are used as adsorbents to trap or hold atoms, ions, and liquids or

dissolved solids on the surface known as adsorbate (Gomez et al. 1996). The most attractive adsorbents are activated carbons due to their low manufacturing cost, variety of raw materials that can be used to obtain activated carbon, high adsorption capacity, high mechanical resistance, high concentration of active sites, proper distribution of pores, variable nature, and quantity of superficial chemical groups. With the previous characteristics and the current global environmental problem of waste tire. Cities of the world generate about 1.3 billion tonnes of tire waste per year. This volume is expected to increase to 2.2 billion tonnes by 2025 (Passaponti et al. 2019; Pedram et al. 2017), and much of it ends up in sidewalks, wetlands, and parks, causing health problems. One solution could be to use these waste tires as a resource to produce activated carbon, which can then be used to remove Triton X-100 from waterways. This research focuses on the production of activated carbon by chemical activation from tire waste tire that allows efficient removal of Triton X-100 from an aqueous solution.

2 Experimental methods

2.1 Treatment of waste tires

Tires were collected in a factory that picks them up for disposal. The tires were cleaned with pressurized air in order to remove adhering solids. These were then cut into an approximate size of 500 mm and passed through a grinding process. The grinding was done in a blade mill of local construction until obtaining a particle size of approximately 0.3 mm. During the process of grinding with a magnetic medium, the steel was removed, so that only the rubber of the tire remained. The rubber was then subjected to a chemical activation process.

2.2 Chemical activation

The chemical activation was carried out at different concentrations of potassium hydroxide (10, 20, 30, and 40% w-w⁻¹), this is called impregnation in was done in a solution with a ratio KOH/waste tire of 1.5:1 w-w⁻¹. Impregnation with the activating agent was carried out for 48 h with constant stirring. Subsequently the solid was dried at 110 °C for 24 h. Then, the impregnated samples are taken to a carbonization process at a heating rate of 2 °C·min⁻¹ with a N₂ flow 100 mL·min⁻¹, until the desired activation temperature was reached (700 °C and 900 °C) and held at that temperature for 3 h in a horizontal Carbolite™ oven. With this procedure eight carbons were obtained, which were labeled as follows: QK107, where Q means chemical activation, K means potassium hydroxide, 10 means 10% potassium hydroxide and 7 means 700 °C. Once the activated carbon was obtained, it

was washed with 0.1 M hydrochloric acid and then water at 60 °C until constant pH value was obtained (Torrado et al. 2011).

2.3 Characterization of activated carbons

The textural characterization of the porous solids was carried out by N₂ physical adsorption at –196 °C, using Quantachrome equipment, Autosorb iQ2 with ASIQwin software. About 0.100 g of sample were weighted and degassed at 200 °C for a period of 3 h at 10^{–3} Torr. Once the degassing process was completed, the analysis was carried out. Apparent A_{BET} surface areas, micropore volume, mesopore volume, and pore distribution were determined.

The experimental results of adsorption–desorption isotherms of N₂ at –196 °C were analyzed in different pressure ranges, using the method of Brunauer, Emmett and Teller (BET) for the calculation of apparent surface areas. The micropore BET assistant were used to define the range of P·P₀^{–1} relative pressures in which the equation can be applied 0.01–0.2. The BET equation is applied in Eq. (1) (Brunauer et al. 1938).

$$\frac{P}{V * (P^0 - P)} = \frac{1}{V_m * C} + \frac{C - 1}{V_m * C} * \frac{P}{P^0} \quad (1)$$

where P is the equilibrium vapor pressure, P₀ is the saturation vapor pressure of the gas that is adsorbed, C means a constant that involves the adsorption heat of the first layer, with the heat released when the second layer is formed, V is the amount adsorbed in volume and V_m is the monolayer volume at normal conditions.

Later, P·(V (P₀ – P))^{–1} versus P·P₀^{–1} should give a straight line, being the slope V_m and the intercept C. For the case of activated carbons, the linearity interval is limited to relative pressures between 0.01–0.20.

The surface area S_{BET} per unit mass of sample is calculated as shown in Eq. (2). S_{BET} is the surface of the solid, V_m is the measure of the capacity of the monolayer, A_m is the area occupied by each molecule, M the molecular weight of the adsorbate and N_{AV} the number of Avogadro (Rouquerol et al. 1999).

$$S_{BET} = \frac{V_m}{M} * N_{AV} + A_m * 10^{-20} \quad (2)$$

Finally, the total volume of pores V_t, was calculated from the volume adsorbed at the relative pressure of 0.99, and the volume of mesopores by difference. The microporosity analysis is performed by the Dubinin - Astakhov model (a P·P₀ < 0.1) (Rouquerol et al. 1999).

In the chemical characterization, chemical surface functional groups were identified using an infrared spectroscopy

technique, which uses a diffuse reflectance cell (Pike-Difuss IR). This was done by means of a Shimadzu IRTracer-100 FT-IR spectrophotometer, performing a scan from 4000 to 400 cm^{–1}, with a resolution of 8 cm^{–1} and 250 scan. For the analysis, the activated carbons were crushed and mixed with KBr in solid-KBr ratio of 1% w·w^{–1}.

Additionally, the Boehm titration method was used to identify functional groups, for which solutions of 0.05 M NaHCO₃, 0.05 M Na₂CO₃, 0.05 M HCl and 0.05 M NaOH were prepared, 50 mL of each solution was measured. Then, 0.100 g of activated carbon was added to each solution. These mixtures were placed in constant stirring for 48 h and then filtered. An aliquot of 5 mL of each filtered solution was taken and processed with the respective titration with NaOH and HCl according to the case (Boehm 2002). In addition, the zero load point was determined. The activated carbon was then weighed between 50 and 500 mg, 10 mL of 0.1 M NaCl was added. These mixtures were placed at 150 rpm for 48 h and then the pH was measured (Yakout 2015). Finally, the thermal decomposition of the eight carbons was obtained by means of a thermogravimetric analyzer (Hitachi, TGA/STA7200). Approximately 10 mg of activated carbon was weighed until this was placed at a heating rate of 5 °C·min^{–1} with a nitrogen flow of 100 mL·min^{–1} until 900 °C.

In the structural characterization, scanning electron microscopy (SEM) was used, by means of the JEOL equipment, model JSM 6490-LV, equipped with a scattered energy X-ray detector (EDS). Prior to the analysis the samples were coated with a layer of gold.

2.4 Adsorption of Triton X-100

The adsorption capacity of Triton X-100 surfactant was determined for a series of eight carbons. Consequently, 0.100 g of activated carbon was weighed and placed with 50 mL of surfactant at different concentrations from 10 mg·L^{–1} to 1000 mg·L^{–1}, including a carbon blank. It was placed at a constant stirring of 100 rpm at a temperature of 18 °C for 7 days, the necessary time to reach the equilibrium point. The solution is then filtered and the amount of non-adsorbed surfactant was measured by high-resolution liquid chromatography at a wavelength of 277 nm, with a column EUROBOND C18 5.0 μm SL-04 (125 × 4.0 mm), and the concentration was determined in the equilibrium Eq. (3). The measurements were duplicated to ensure accuracy. Additionally, the influences of temperature on adsorption of Triton X-100 at three temperatures (18, 35, and 65 °C) were studied.

The amount of triton X-100 absorbed is determined using Eq. (3) where where C₀ and C_e (mg·L^{–1}) are the initial and final concentration of Triton X-100 in the solution, V is the

volume of the solution (L), and m is the mass of activated carbon (g).

$$Q_e = \frac{V(C_0 - C_e)}{m} \quad (3)$$

The adsorption isotherms enable modeling and interpretation of the way in which adsorbents interact with adsorbates at a constant temperature. These models help to establish the adsorption capacity of the adsorbate on the adsorbent and additionally facilitate establishing the possible adsorption mechanisms (Foo and Hameed 2010).

In this study some common isotherms were used to fit the experimental data and to describe and understand the adsorption process at a macroscopic level. The four isotherms were: Langmuir Eq. (4), Freundlich Eq. (5), Toth Eq. (6), and Redlich-Peterson Eq. (7) (Adamson 1990; Talu and Meunier 1996).

2.4.1 Langmuir isotherm model

The Langmuir adsorption isotherm was originally developed to describe gas–solid-phase adsorption on activated carbon by Langmuir (1916). This empirical model assumes monolayer adsorption. The adsorption can only occur at a finite (fixed) number of definite localized sites that are identical and equivalent, with no lateral interaction and steric hindrance between the adsorbed molecules, even on adjacent sites. It may be expressed as in Eq. (4)

$$Q_e = \frac{Q_0 K_L C_e}{1 + K_L C_e} \quad (4)$$

2.4.2 Freundlich isotherm model

The Freundlich adsorption isotherm (Freundlich 1906) is an exponential equation Eq. (5). This empirical model describes the reversible, multilayer adsorption with affinities over the heterogeneous surface and non-uniform distribution of adsorption heat (Foo and Hameed 2010).

$$Q_e = K_F C_e^{1/n} \quad (5)$$

2.4.3 Toth isotherm model

The Toth isotherm model is an empirical model (Toth 1971), which improves the Langmuir isotherm fittings. This describes heterogeneous adsorption systems, for high and low concentrations. It may be expressed as in Eq. (6)

$$Q_e = \frac{K_T C_e}{(a_T + C_e)^{1/t}} \quad (6)$$

2.4.4 Redlich-Peterson isotherm model

The Redlich-Peterson isotherm (Redlich and Peterson 1959) is a union between the model of Langmuir and Freundlich. The model incorporates three parameters, which have a linear dependence on concentration in the numerator and an exponential function in the denominator. In the limit, at high concentrations, it approaches the Freundlich isotherm model (as the exponent tends to zero) and at low concentration to the Langmuir model (as the values are all close to one). It may be expressed as in Eq. (7)

$$Q_e = \frac{K_{RP} C_e}{1 + a_R C_e^B} \quad (7)$$

In these equations, C_e ($\text{mg}\cdot\text{L}^{-1}$) is concentration equilibrium; Q_e ($\text{mg}\cdot\text{g}^{-1}$) is the maximum amount of Triton X-100 adsorbed at equilibrium; Q_0 ($\text{mg}\cdot\text{g}^{-1}$) is the maximum coverage capacity in the monolayer; K_L ($\text{L}\cdot\text{mg}^{-1}$) is the Langmuir constant related to the adsorption energy; K_F ($\text{mg}\cdot\text{g}^{-1}$) is the Freundlich constant; n is an exponent related to the strength of the adsorption; K_T ($\text{mg}\cdot\text{g}^{-1}$), a_T ($\text{L}\cdot\text{mg}^{-1}$), and t are constants of Toth; K_{RP} ($\text{L}\cdot\text{g}^{-1}$), a_R ($\text{L}\cdot\text{g}^{-1}$) are constants of Redlich-Peterson, and B is the exponent of Redlich-Peterson.

3 Results and discussion

3.1 Preparation of activated carbons

Table 1 shows the yields obtained during the preparation of the series of eight activated carbons by chemical impregnation, using potassium hydroxide as the activating agent. The carbonization yields are between 40% and 46%. In the tire pyrolysis process as reported in literature (Rofiqul et al. 2008), there are three stages of thermal decomposition defined by a range in which there is a maximum decomposition. These are: (1) 120–280 °C with a maximum of 256 °C which is associated with the volatilization of plasticizers and dyes, (2) 280–440 °C with a maximum at 380 °C corresponding to the degradation of natural rubber, and (3) 400–520 °C with a maximum at 460 °C where the degradation of synthetic rubber occurs (Miranda et al. 2006). These stages were obtained in the thermogravimetric analysis that was carried out experimentally, as shown in Fig. 2. Generating three types of products: solids, liquids and gasses whose percentage varies depending on the conditions of pyrolysis. According to studies of the decomposition, Xylene was obtained by the decomposition of natural rubber. In contrast, the aromatic components (isopropene dimer, ethylbenzene, styrene and cumene) were mainly caused by the decomposition of the styrene fraction in synthetic rubber (Seidelt

Table 1 Textural properties of the activated carbon (Dubinin Astakov) and yield in the carbonization process

Sample	Yield (g _{CA} /100g _{tire})	BET		Dubinin Astakov				V _{meso} (cm ³ ·g ⁻¹)
		S _{BET} (m ² ·g ⁻¹)	C	V _{micro} (cm ³ ·g ⁻¹)	E ₀ (kJ·mol ⁻¹)	n	Pore width (Å)	
QK107	46	54	211	0.019	5.663	2.3	7.9	0.31
QK109	43	67	216	0.022	5.602	2.6	8.0	0.46
QK207	42	46	215	0.016	5.846	2.3	7.8	0.31
QK209	41	55	280	0.020	6.346	1.9	7.5	0.33
QK307	41	89	380	0.033	6.293	2.1	7.6	0.39
QK309	40	528	770	0.198	7.093	2.2	7.3	0.51
QK407	40	263	1182	0.101	7.926	1.9	7.0	0.54
QK409	40	426	680	0.157	6.942	2.3	7.4	0.67

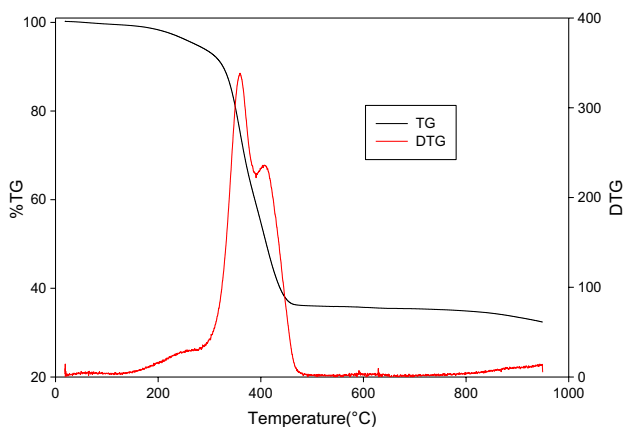
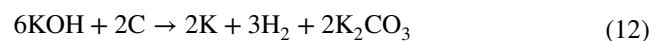


Fig. 2 Thermograms for waste tire obtained at 5 °C min⁻¹ with a nitrogen flow of 100 mL·min⁻¹

et al. 2006). These percentages of yield (Table 1) were high compared to what was reported in the literature, where percentages the production of solids 25%, liquids 48% and gases 26% are found (Betancur et al. 2009). Another study reports 25% in the production of solids (Teng et al. 2000) and according to Cardona et al. (2015) the percentage of performance are 22% solids, 48% liquids, and 30% gases. As previously mentioned, the percentage of yield for the solids obtained in this research is between 40% and 46%. These values differ significantly from what it was reported in the literature, this can be attributed to the residence time of the solid inside the reactor, the heating rate, the amount of sample and the differences present in the raw material used. Furthermore, it is evident in Table 1 that as the production of solids is reduced, the BET area increases and contributes to the formation of the porosity. This is also reported by some authors. Teng et al. 2000, using KOH/Tire ratio of four impregnating agent found that when increasing the pyrolysis temperature from 600 to 700 °C, the carbon yield decreases (26% to 16%) and increases the BET area (116 to 474 m²·g⁻¹). Additionally, Betancur et al. 2009 performed

a study with physical activation finding in the same way that it has higher temperature (800 to 900 °C), lower yield (36.4 to 32.9%) and greater BET area (4.46 to 82.18 m²·g⁻¹). Cardona et al. 2015 using impregnating agent KOH, H₃PO₄ and ZnCl₂ where up to a yield of 9% is obtained with an area of 1260 m²·g⁻¹.

Otherwise, the decrease in yield percentages by increasing the concentration of impregnating agent and the pyrolysis temperature may be due to the increase in carbon gasification. The reaction process between impregnation agent and carbonaceous sample consists of a series of simultaneous reactions, shown in Eqs. (8–16). The potassium hydroxide (KOH) dehydrates to form a potassium oxide (K₂O) at 400° C in Eq. (8). Subsequently, carbon reacts with water and produces carbon oxide (CO) and hydrogen Eq. (9). Then, carbon oxide with water reacts to produce carbon dioxide in Eq. (10). This carbon dioxide reacts with potassium oxide to form potassium carbonate (K₂CO₃), as shown in Eq. (11). Potassium carbonate is decomposed into carbon oxide and carbon dioxide at a temperature higher than 700 °C Eq. (13) at temperatures and higher than 800 °C decomposes completely. Additionally, CO₂ can be reduced to CO Eq. (14) and K₂O and K₂CO₃ Eqs. (15, 16) can be reduced by carbon, producing metallic potassium at temperatures above 700 °C (Otowa et al. 1993; Ahmadpour and Do 1996).



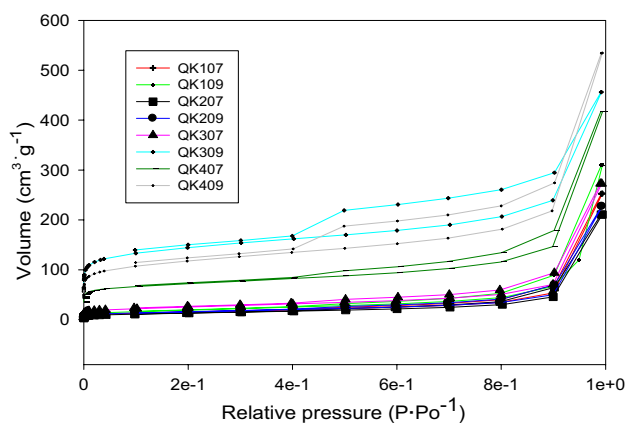


Fig. 3 Adsorption-desorption isotherms of N_2 at -196 °C for the series of activated carbons



3.2 Characterization of activated carbons

3.2.1 Characterization of the physical structure

The structural characterization of the activated carbons was determined by means of N_2 adsorption isotherms at -196 °C. Figure 3 shows the obtained isotherms corresponding to each of the prepared carbons, where according to the classification stipulated by the IUPAC (Thommes et al. 2015), the classification corresponds to isotherms type IV(a), which are characteristic of mesoporous adsorbents where the adsorption behavior in mesopores are determined by adsorptive-adsorptive interactions and by interactions between molecules in the condensed state. The initial monolayer-multilayer adsorption occurs in the walls of the mesopores in the same way as an isotherm type II, and can be observed in is subsequently given by the condensation of pores. This capillary condensation is accompanied by a hysteresis loop, type H4, which occurs in micro-mesoporous carbons. This behavior is observed for all prepared activated carbons. Additionally, as the concentration of impregnating agent increases, the adsorption capacity increases as well as the temperature at the same concentration, and an increase in the adsorption capacity is seen. Despite being characteristic isotherms for mesoporous materials, some adsorption has been observed at very low relative pressures ($P \cdot P_0^{-1} < 0.1$), which is attributed to the presence of a certain degree of microporosity.

In Table 1, is observed that the carbons whose final temperature was 900 °C have a greater BET area with respect to those of 700 °C. Since a greater interaction with

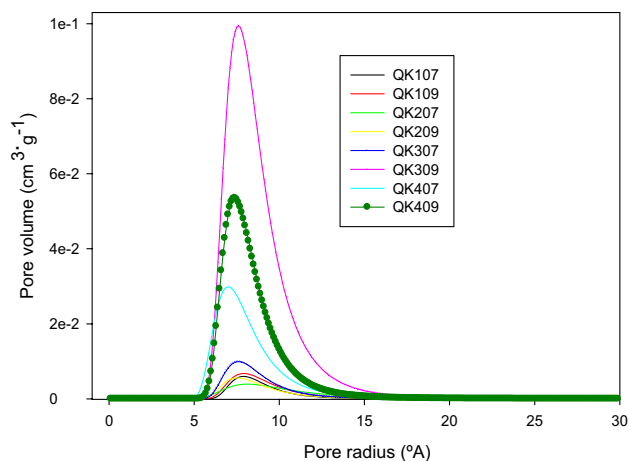


Fig. 4 Pore size distribution by Dubinin-Astakhov

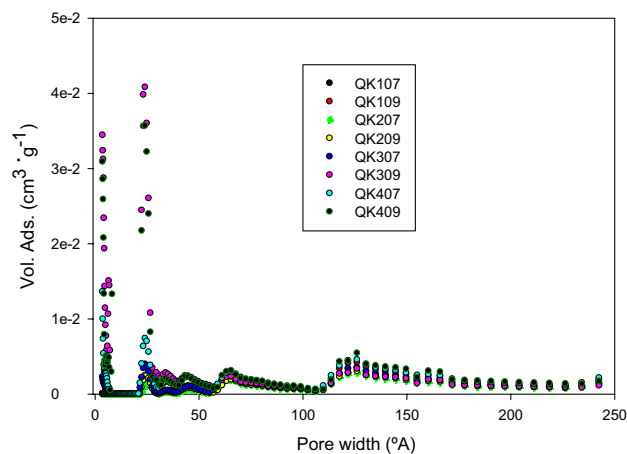


Fig. 5 Pore-size distributions with hybrid slit/cylinder adsorption branch quenched solid density functional theory (QSDFT) kernels for activated carbon

the precursor takes place, attacking the matrix, the areas between the range of $46\text{--}528$ $m^2 \cdot g^{-1}$ are obtained. Additionally, a pore average of 7.0 to 8.0 Å in Fig. 4 is obtained by Dubinin-Astakhov. Regarding the mesoporous volume, at higher concentrations of potassium hydroxide, greater mesoporosity is generated, evidencing the greatest mesoporous volume at 0.67 $cm^3 \cdot g^{-1}$. This may be due to the fact that temperatures above 700 °C K_2O and K_2CO_3 Eqs. (15, 16) can be reduced by carbon to metallic potassium, generating a potassium intercalation in the carbon network and with it an improvement in the porosity (Otowa et al. 1993; Wang and Kaskel 2012).

Pore size distribution was determined by quenched solid density functional theory (QSDFT) model. It was based on the hybrid kernels of adsorption branch isotherm (Slit-cylindrical) (Lippens et al. 1964), using the ASQiWin software.

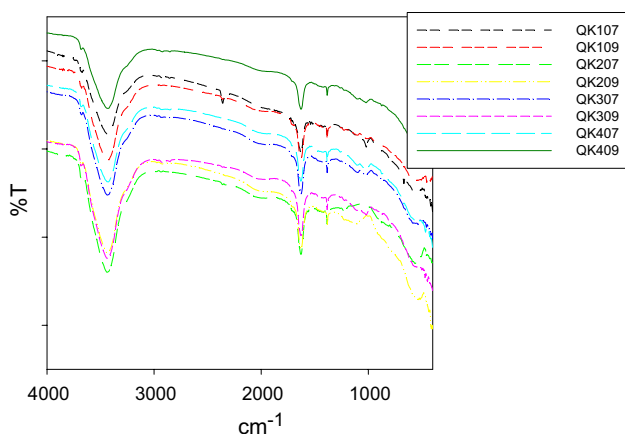


Fig. 6 FT-IR of carbonaceous materials

Table 2 Quantification of acidic and basic surface groups by the Boehm’s titration method

Sample	Basic groups (meq·g ⁻¹)	Carboxylic groups (meq·g ⁻¹)	Lactonic groups (meq·g ⁻¹)	Phenolic groups (meq·g ⁻¹)	pHpzc
QK107	0.395	0.881	1.310	2.115	7.5
QK109	0.587	1.211	1.150	0.556	7.5
QK207	0.586	1.243	1.090	1.523	7.6
QK209	0.619	1.474	1.070	2.772	7.7
QK307	0.627	0.997	0.040	0.678	8.0
QK309	0.627	1.510	1.040	1.667	8.5
QK407	0.670	1.900	1.300	1.460	8.6
QK409	0.870	1.456	0.910	0.392	8.8

In Fig. 5 a pore size distribution between 5 and 150°A for each of the prepared carbons is observed. The greater the percentage of impregnation agent, the greater the volume adsorbed and the lower percentage of yield (Table 1). These results can be correlated, since the CO₂ formed as explained in item 3.1 Eqs. (8–16) reacts with the carbon atoms to open the closed pores and expand the existing micropores, it is increasing porosity. In addition to the formation of CO₂ at a higher temperature than 700 °C, K₂O and K₂CO₃ Eqs. (8–16) (Di et al. 2009) cause the gasification of carbon and its oxidation. Besides, the metal K formed at high temperatures can intercalate with the carbon matrix increasing the volume of pores, and with a severe thermal treatment, causes the breakage of cross-links in the carbon matrix, producing a reorganization of the carbonaceous aggregates and collapse of the pores.

3.2.2 Chemical characterization

FT-IR infrared spectra of the activated carbons are shown in Fig. 6. Four bands were seen at 3430, 1633, 1388 and 1092 cm⁻¹ all of which can be assigned to O–H, C=O, C–H bending, C–C, and S=O. The S=O was due to the standard

vulcanization process and it was associated to the band at 490 cm⁻¹ of low intensity, characteristic of S–S bond, implying that the thermal treatment carried out with N₂ at 700 and 900 °C affected the sulfur atoms and their bonds (Stuart 2004).

The characterization of the surface groups for the different carbons was also carried out (shown in Table 2) by means of Boehm’s titration method. There wasn’t an appreciable pH variation during the experimentation, remaining between 5 and 7. The acid type groups analyzed were: carboxylic, lactonic and phenolic. The basics groups were considered as the total basics. Table 2 shows that the concentration of basic groups was between 0.3 and 0.9 meq·g⁻¹, which rose with increasing the concentration of activating agent; acid groups were between 0.9 and 1.7 meq·g⁻¹ and there was no evidence of a tendency with the increase of the

activating agent concentration and pyrolysis temperature. The concentration of acid groups correlates with the pH_{pzc} where, as the temperature increased the hydrophobic nature of the carbonaceous materials increases too.

Additionally, the eight carbons obtained were subjected to a thermogravimetric analysis. The thermograms of the activated carbons are shown in Fig. 7 where a maximum loss of 20% w·w⁻¹ was evidenced, showing high thermal stability and low carbon degradation. Below 100 °C there was a small weight loss of approximately 5% w·w⁻¹ for all carbons due to the desorption of physisorbed water, associated with the degree of hydrophobicity and the pore structures (Kim et al. 1995; Fazara et al. 2014). A loss of 2% observed at a temperature among 100–250 °C, it was attributed to decomposition of surface functional groups of low stability, generated upon activation and finally, a weight loss of 13% above 250 °C that which could associated with the decomposition of functional groups and to partial gasification of the least thermally stable fragments of the carbon matrix (Miguel et al. 1998; Bazan et al. 2016).

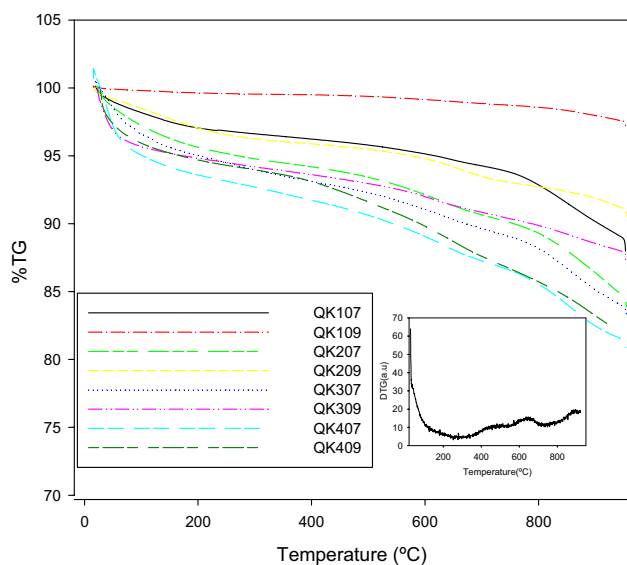


Fig. 7 Thermograms for the activated carbons obtained at $5\text{ }^{\circ}\text{C}\cdot\text{min}^{-1}$ with a nitrogen flow of $100\text{ mL}\cdot\text{min}^{-1}$

3.2.3 Structural characterization

In order to know the morphology of the activated carbons that were prepared, an analysis by scanning electron microscopy was carried out. Additionally, an X-ray detector with dispersed energy (EDS) was used in order to know the composition of the activated carbons. Figure 8 shows the images for the external surface of activated carbons in micrometric scale. A heterogeneous grain distribution was observed in all the micrographs, which presents cavities with a high degree of roughness.

Although micropores and mesopores are not visible, photographs showed the shapes and location of the macropores on the surface of the solid.

Furthermore, the development of the pore distribution is explained in two steps: micropores were created and then some micropores became wider to produce larger pores known as mesopores. Additionally, there were macropores that were formed during activation by the effect of the impregnating agent and the loss of volatile matter during

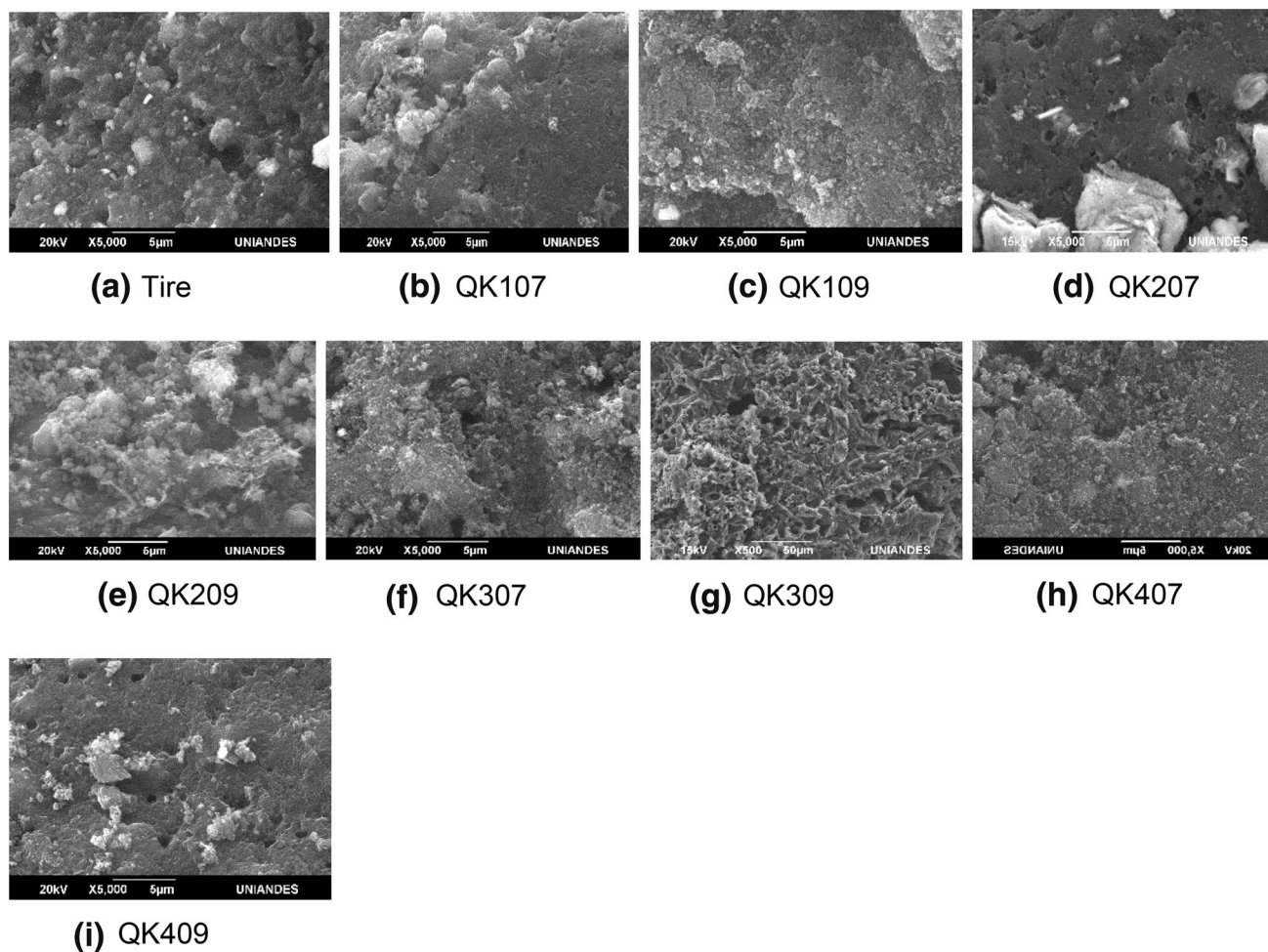


Fig. 8 Electron micrographs of the series of the eight activated carbons QK107 (a), QK109 (b), QK207 (c), QK209 (d), QK307(e), QK309 (f), QK407 (g), and QK409 (h); taken at an magnification of 5000X

Table 3 Elements found in the eight activated carbons by the Energy-Dispersive X-Ray Spectroscopy (EDS)

Element	QK107 Atomic %	QK109 Atomic %	QK207 Atomic %	QK209 Atomic %	QK307 Atomic %	QK309 Atomic %	QK407 Atomic %	QK409 Atomic %
C	78.82	77.22	78.82	80.38	81.10	88.96	82.93	93.81
O	14.28	15.47	14.28	16.05	13.61	9.06	12.72	4.57
Al	0.54	0.55	0.54	0.12	0.22	0.19	0.60	0.07
Si	2.49	2.41	2.55	1.41	2.17	0.83	1.45	0.76
S	1.13	0.91	1.13	0.18	0.59	0.45	0.79	0.19
Ca	0.95	0.98	0.84	0.90	0.44	0.52	–	0.19
Fe	0.32	0.29	0.32	0.39	0.09	–	0.21	0.10
Zn	1.55	2.17	1.52	0.34	1.77	–	0.68	–

Table 4 Adsorption parameters of triton X-100 on activated carbon, using two-parameter models

Sample	Two-parameter adjustment models.					
	Langmuir			Freundlich		
	K_L	Q_0 (mg·g ⁻¹)	R^2	K_f (L·g ⁻¹)	n	R^2
QK107	0.0202	130	0.988	15.0	2.9	0.967
QK207	0.0143	92	0.919	8.26	2.7	0.931
QK307	0.0155	141	0.919	18.7	3.2	0.945
QK407	0.0139	179	0.879	29.4	3.7	0.876
QK109	0.0133	168	0.952	16.4	2.8	0.967
QK209	0.0245	116	0.855	25.3	4.3	0.931
QK309	0.0694	191	0.970	33.6	3.4	0.902
QK409	0.0280	220	0.839	52.7	4.4	0.909
QK409 35 °C	0.186	146	0.933	50.7	5.1	0.951
QK409 65 °C	0.823	158	0.890	99.6	11.1	0.890
QK309 35 °C	0.384	189	0.879	78.3	6.11	0.934
QK309 65 °C	0.826	190	0.782	136	17.1	0.783

pyrolysis favoring diffusional processes (Achaw 2012). Additionally, an increase in roughness was observed when increasing the pyrolysis temperature and the concentration of activating agent (%KOH), where the treatment with potassium hydroxide at 30% w.w⁻¹ generated the sample with the highest porosity and the highest modification to the surface; on the other hand, regarding to thermal modification, 900 °C is the pyrolysis temperature that generated the highest value for the surface area: 528 m²·g⁻¹, according to BET model determination.

The elemental composition on the surface, determined by the Energy- Dispersive X-Ray Spectroscopy (EDS) showed the presence of different elements in addition to carbon, such as silicon, iron, sulfur, aluminum, calcium, and zinc (Table 3). Silicon had the highest relative percentage with respect to the other metals and its composition in activated carbon decreases as the pyrolysis temperature increases too. With respect to the other elements, there was no evidence of a tendency regarding to the composition and pyrolysis temperature. The presence of inorganic compounds may be

associated with rubber additives such as silicon, aluminum, and zinc.

3.3 Adsorption of Triton X-100

After the characterization of the porous solids, the adsorption studies of the pollutant of interest for the decontamination of wastewater were performed. To do this, once the concentration in equilibrium was determined, the data were adjusted to adsorption models of two and three parameters, in order to elucidate how the adsorption of triton X-100 for each of the activated carbons obtained from tire waste was carried out. The adsorption parameters of triton X-100 using the two-parameter models of Langmuir (Langmuir 1918) and Freundlich (Freundlich 1906) are shown in Table 4. Where Q_0 represented the adsorption capacity of activated carbon and n it was directly related to the affinity of the sample for the adsorbate (Freundlich 1906). The adsorption parameters listed in Table 4 revealed a significant improvement in the adsorption capacity of triton X-100 from 92 to 220 mg·g⁻¹ corresponding to the sample treated

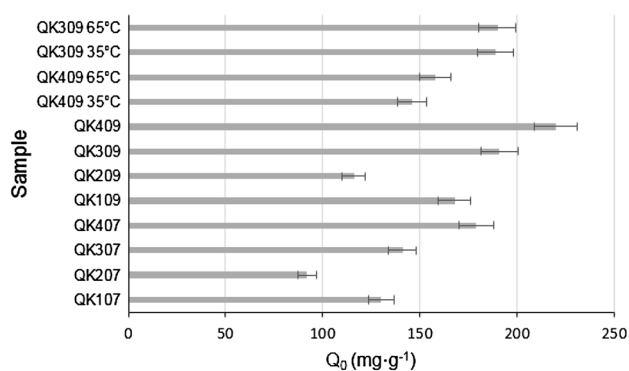
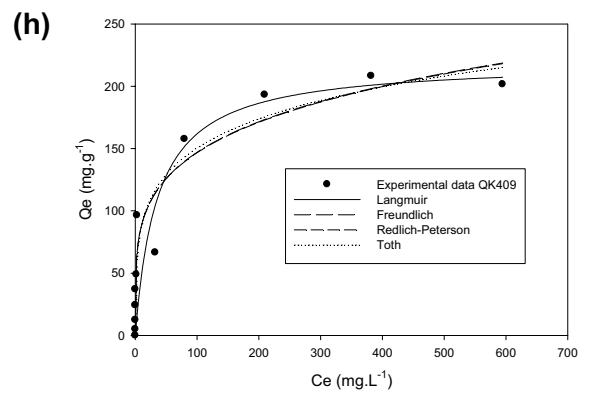
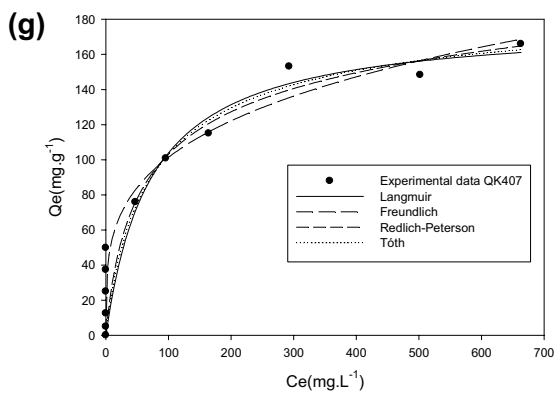
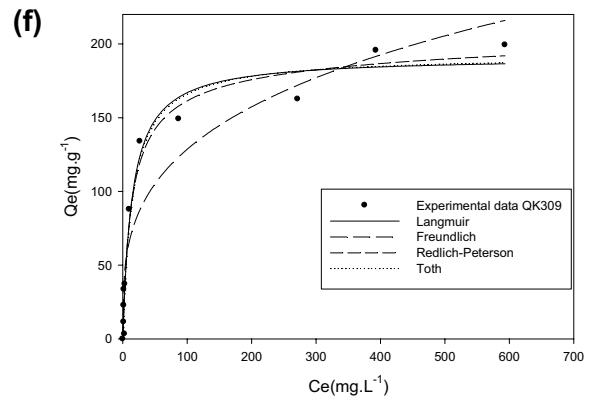
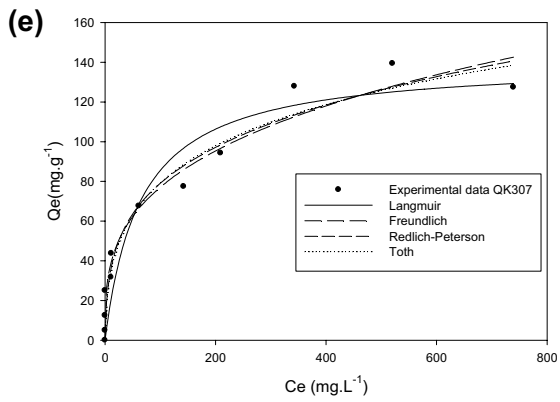
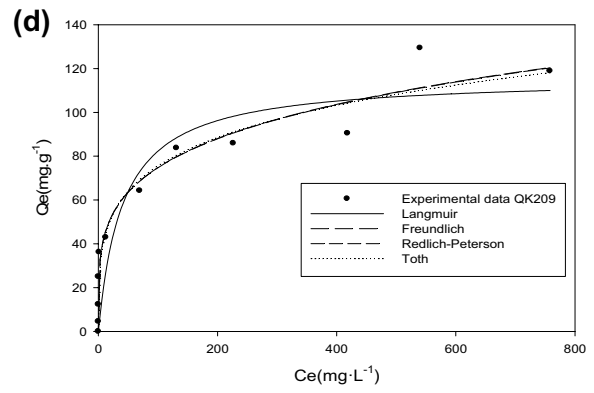
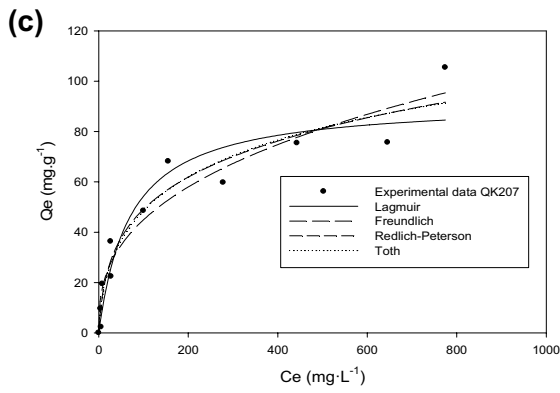
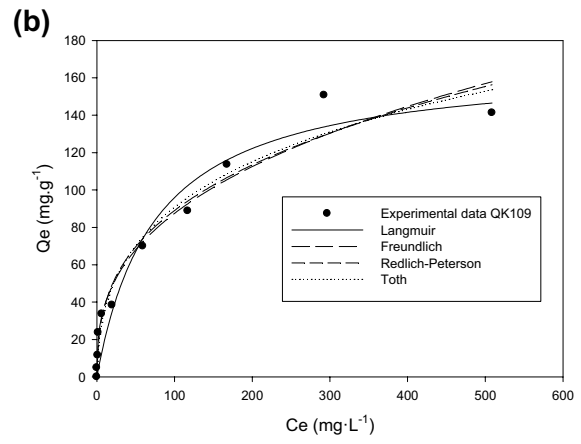
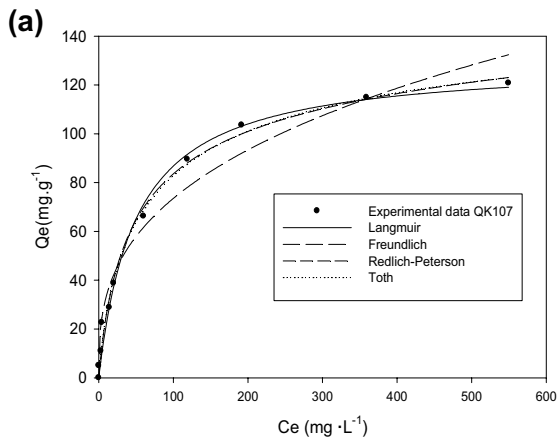


Fig. 9 Parameter of Langmuir model (Q_0) for prepared activated carbons

with KOH at 40% w.w⁻¹ and 900 °C (Figs. 9, 10, 11) where the concentration of impregnate and the temperature of pyrolysis were increased. This could be attributed to higher concentration of impregnating agent which increased the adsorption volume (Figs. 3, 4, 5) throughout the entire pore distribution; but a considerable increase is evidenced at less than 30 Å, which corresponded to the average size of triton X-100. Additionally, there was an increase in the BET area generating a greater number of active sites and with this, the triton X-100 was more easily adsorbed. It was also observed that at a higher concentration of the impregnating agent the carbons presented more basic character favoring the adsorption of triton X-100. All previous parameters favored the adsorption mechanism of triton X-100 on activated carbon. The adsorption process had three steps: first, there was a process of diffusion of triton X-100 through the surface of activated carbon; the second step was the transport of triton X-100 on the surface of activated carbon; the final step was adsorption of triton X-100 inside of the pore and on the surface (Paria and Khilar 2004). Figure 10 showed that the adsorption of the triton X-100 increased when the concentration of the pollutant became higher which implied that the adsorbed molecules the fixation of the surfactant through the interaction of surfactants. Additionally, at the beginning of the Fig. 10 a rapid increase was observed, which indicated the high affinity of the adsorbent for the adsorbate. However, the active sites of the adsorbent were filled, which hindered the adsorption process. Additionally, as the adsorption isotherms were adjusted to models of two parameters such as Langmuir and Freundlich, those were compared with respect to the correlation coefficient (R^2). It was found that for some samples Langmuir was the best-fitting model, while for others it was Freundlich, implying that the adsorption of triton X-100 involved active sites of adsorption with variable energy and that the solids had heterogeneous surface. Regarding to the parameter n ,

Fig. 10 Representation of adjusted adsorption models of triton X-100 adsorption on the eight-carbon series at 18 °C: QK107 (a), QK109 (b), QK207 (c), QK209 (d), QK307 (e), QK309 (f), QK407 (g), and QK409 (h)

values greater than one ($n > 1$), were observed which demonstrated that activated carbon had a high affinity for the triton X-100 molecules. Additionally, increasing n implied a greater affinity between triton X-100 and activated carbon, while $1/n = 1$ indicated a linear adsorption leading to identical adsorption energies for all sites. With respect to the adsorbed amount, it was found that by increasing the concentration of triton X-100, the amount of surfactant was removed reached a maximum concentration of 100 mg·L⁻¹ (Fig. 9), where the adsorbed amount (q_e) increases rapidly. It was attributed to a greater interaction between the adsorbent and the molecules of surfactant due to the increase in the motive force of the concentration gradient. After this concentration (up to 1000 mg·L⁻¹) a constant adsorption value was reached, because at higher concentration there was greater agglomeration of adsorbate particles on the surface of the adsorbent and this decreased the availability of active sites for the adsorption sites in the adsorbent, until the point of saturation of these available sites on the activated carbon surface. This type of isotherm resembled type H according to the classification made by Giles et al. (1960) which suggested that there was high affinity between the adsorbent and the adsorbate and that the solutions at low concentrations are completely adsorbed (< 100 mg·L⁻¹) or there was small measurable amount left in the solution, so the initial part of the isotherm was almost vertical. With respect to the equilibrium time, the slow rate of adsorption of TX-100 was probably due to the slow diffusion of the surfactant into the pores of the adsorbent (Yakout and Nayl 2009). This depended on the dimensions of the surfactant, where at concentrations lower than 600 mg·L⁻¹, it was found as monomer and at concentrations higher than 600 mg·L⁻¹ it was found as binder (Fig. 12). In these cases, a small variation in the concentration of the surfactant could cause a big effect on the adsorption. This was because depending on adsorbate–adsorbate and adsorbate–solvent interactions, the aggregation of the surfactant changed its orientation and packing on the surface. Figure 12 shows a diagram of the most probable changes in the orientation and in the adsorption of a nonionic surfactant on the surface of the solid, thus causing a greater or lesser adsorption depending on the pore size and its accessibility (Paria and Khilar 2004). Adsorption of Triton X-100 occurred at the hydrophilic solids interface below the micellar concentration. For the process of adsorption of the non-ionic surfactant, three processes could occur in the solution depending on the concentration: monomer diffusion (lower



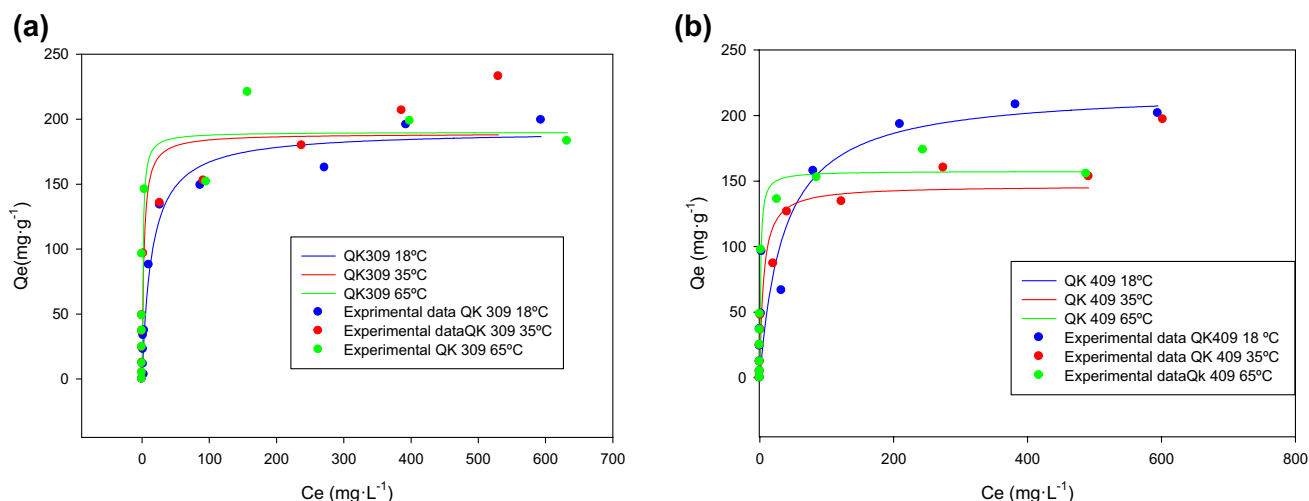


Fig. 11 Representation of adjusted adsorption models for triton X-100 adsorption on activated carbons QK 309 (a), and QK409 (b) at different temperatures

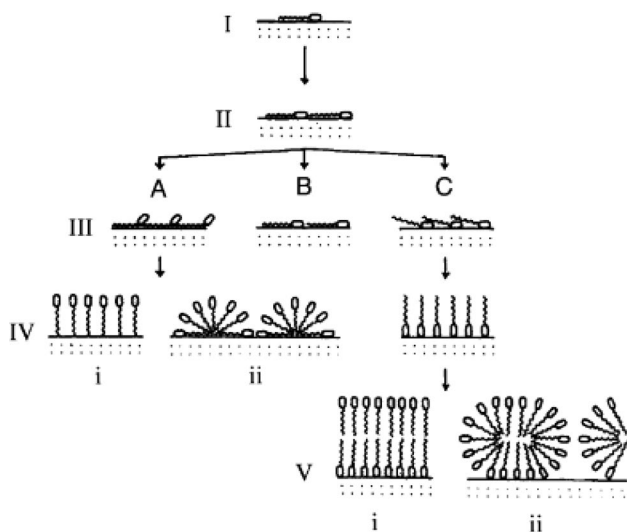


Fig. 12 Diagram of the most probable changes in orientation for the adsorption of a nonionic surfactant on the surface of the solid (Paria and Khilar 2004)

concentration to the micellar one: $600 \text{ mg}\cdot\text{L}^{-1}$), micellar diffusion ($600 \text{ mg}\cdot\text{L}^{-1}$) and micellar dissociation.

On the other hand, the data of the isotherms could be explained by three-parameter models (Table 5), the Redlich-Peterson model incorporated the characteristics of the Langmuir and Freundlich isotherms, since the parameter b was close to one, the equation tended towards the Langmuir isotherm; therefore, it could be concluded that the experimental results fitted properly to the Langmuir model. In the Redlich-Peterson model, the adsorption mechanism was a

hybrid and did not follow the ideal adsorption in monolayer. In the case of the Toth model, the parameter T represented heterogeneity, since it was different from 1. The Toth model is applied to heterogeneous systems and is derived from the potential theory, it also assumes a quasi-Gaussian energy distribution, meaning that most sites have a lower energy with respect to the maximum energy of adsorption, this is consistent taking into account that the surface of a carbonaceous porous solid and/or modified is of heterogeneous due to the chemical nature of the surface exposed to the adsorbate molecules.

Finally, when increasing the temperature to 35°C and 65°C (Table 4), for QK309 there was no significant increase in the adsorption capacity; meanwhile for QK409 the capacity of adsorption increased with the temperature, so adsorption of Triton X-100 on QK409 was dependent on the temperature. This could be interpreted as that the increase in temperature increased the collision frequency and favored the diffusion of TX-100 from the solution to the activated carbon surface.

When comparing these results with the literature, there aren't references related to the adsorption of Triton X-100 on carbonaceous materials obtained from tire waste; therefore, the comparison was made with a system of triton X-100 adsorbed on carbon obtained from coconut husk, where the Q_0 was $194 \text{ mg}\cdot\text{g}^{-1}$. In contrast, the amount adsorbed (Q_0) of this pollutant on the solid obtained in this work was $220 \text{ mg}\cdot\text{g}^{-1}$, which is remarkable considering that this was a complicated matrix to develop porosity and surface area, taking into account that this carbon derived from rubber (Zahoor 2016).

Table 5 Adjustment parameters of Triton X100 adsorption isotherms using three-parameter models

Sample	Three-parameter models							
	Redlich-Peterson				Toth			
	K_{RP} (L·g ⁻¹)	(L·mg ⁻¹)	b	R ²	K_T (mg·g ⁻¹)	a_T (L·mg ⁻¹)	T	R ²
QK107	3.61	0.055	0.890	0.991	161	7.97	0.604	0.993
QK207	3.43	0.186	0.754	0.942	238	2.36	0.297	0.934
QK307	15.6	0.644	0.732	0.946	531	1.21	0.204	0.947
QK407	4.02	0.051	0.875	0.880	193	23.8	0.788	0.880
QK109	35.9	1.847	0.664	0.968	955	1.32	0.188	0.970
QK209	3.0 × 10 ⁵	11749	0.765	0.931	3284	0.419	0.070	0.927
QK309	15.1	0.103	0.954	0.972	193	12.3	0.953	0.970
QK409	1.4 × 10 ⁵	2683	0.777	0.909	2068	0.416	0.092	0.907
QK 409 35 °C	80.2	1.083	0.873	0.965	216	0.737	0.321	0.967
QK 409 65 °C	219	1.763	0.953	0.894	180	0.322	0.367	0.895
QK309 35 °C	1.3 × 10 ⁶	16486	0.836	0.935	1041	0.273	0.091	0.931
QK309 65 °C	395	2.598	0.961	0.784	197	0.234	0.452	0.783

4 Conclusions

The tire was subjected to a chemical impregnation with potassium hydroxide and later carbonization. The BET surface areas were between 42 and 528 m²·g⁻¹ with micro/mesoporous structure. It was found that variations in impregnation concentration and pyrolysis temperatures had a significant effect on the development of porosity. The adsorption isotherms showed that higher pyrolysis temperatures favored the development of porosity. Additionally, the process of adsorption of Triton X-100 was favored with the increase of the concentration of the activating agent and with the increase of the carbonization temperature. Finally, a higher percentage of Triton X-100 was adsorbed at concentrations lower than 100 ppm.

Acknowledgements The authors would like to thank to the Research and Postgraduate Committee-Faculty of Sciences of the Universidad de los Andes, Colombia for the funding of research projects and the presentation of results in academic events in 2018-1, according to the project “Obtaining of activated carbon for the decontamination of surfactant in wastewater”. The authors also appreciate the grant for the funding of research programs for Associate Professors, Full Professors, and Emeritus Professors announced by the Faculty of Sciences of the University of the Andes, 20-12-2019-2020, 2019, according to the project “Enthalpy, free energy and adsorption energy of the activated carbon interaction and solutions of emerging organic compounds”.

References

- Abd-allah, A., Srorr, T.: Biodegradation of anionic surfactants in the presence of organic contaminants. *Water Res.* **32**(3), 944–947 (1998)
- Achaw, O.W.: A Study of the Porosity of Activated Carbons Using the Scanning Electron Microscope. *Scanning Electron Microscopy*, pp. 473–490. Intech, Rijeka (2012)

- Adamson, A.: *Physical Chemistry of Surfaces*. Wiley, New York (1990)
- Ahmadpour, A., Do, D.: The preparation of active carbons from coal by chemical and physical activation. *Carbon* **34**(4), 471–479 (1996)
- Bazan, A., Nowicki, P., Pórolniczak, P., Pietrzak, R.: Thermal analysis of activated carbon obtained from residue after supercritical extraction of hops. *J. Therm. Anal. Calorim.* **125**(3), 1199–1204 (2016)
- Betancur, M., Martínez, J., Murillo, R.: Production of activated carbon by waste tire thermochemical. *J. Hazard. Mater.* **168**, 882–887 (2009)
- Boehm, H.: Surface oxides on carbon and their analysis: a critical assessment. *Carbon* **40**, 145–149 (2002)
- Brunauer, S., Emmett, P., Teller, E.: Adsorption of gases in multimolecular layers. *J. Am. Chem. Soc.* **60**(2), 309–319 (1938)
- Cardona, L., Betancur, M., Martínez, J.: Transformación termoquímica de neumáticos usados en una sola etapa en atmósfera de CO₂ para la obtención de carbón activado y comparación con el obtenido en dos etapas. *Revista Investigaciones Aplicadas.* **9**, 57–69 (2015)
- Datta, M., Fenton, J., Broomam, E.: *Environmental aspects of electrochemical technology: Applications in electronics*, Ilustrada (1997)
- Di, C., Galgano, A., Branca, C.: Effects of potassium hydroxide impregnation on wood pyrolysis. *Energy Fuels* **23**, 1045–1054 (2009)
- Dinesh, M.: *Water Policy Science and Politics*. Elsevier, India (2018)
- Fazara, U., Jainoo, M., Ismail, K., Hussin, K., Fahmi, M.: Physico-chemical properties of pyrolytic carbon black from waste tyres. *Key Eng. Mater.* **182**, 178–182 (2014)
- Fazley, M., Wang, F., Li, Y., Wang, L.: *Porous Structures from Biobased Synthetic Polymers via Freeze-Drying*. Springer, Germany (2017)
- Foo, K., Hameed, B.: Insights into the modeling of adsorption isotherm systems. *Chem. Eng. J.* **156**(1), 2–10 (2010)
- Freundlich, H.: Over the adsorption in solution. *J. Phys. Chem.* **57**, 385–471 (1906)
- Giles, C., MacEwan, T., Nakhwa, S., Smith, D.: Studies in adsorption. Part XI. A system of classification of solution adsorption isotherms, and its use in diagnosis of adsorption mechanisms and in measurement of specific surface areas of solids. *J. Chem. Soc.* **14**, 3973–3993 (1960)
- Gomez, I., Garcia, M., Salinas, C., Linares, C.: Activated carbons from spanish coal. 2. Chemical activation. *Energy Fuels* **10**, 1108 (1996)
- Jiménez, A., Salazar, M., Gutiérrez, M., Monroy, O.: Anaerobic digestion of a nonionic surfactant: inhibition effect and biodegradation. *Water Sci. Technol.* **44**(4), 175–181 (2001)

- Johnson, M.: Detergents: Triton X-100, Tween-20. *Mater. Methods* **3**, 163 (2013)
- Kim, S., Park, J., Chun, H.: Pyrolysis kinetics of scrap tire rubbers. I: using DTG and TGA. *J. Environ. Eng.* **121**, 507–514 (1995)
- Koley, D., Bard, A.: Triton X-100 concentration effects on membrane permeability of a single HeLa cell by scanning electrochemical microscopy (SECM). *Proc. Natl. Acad. Sci.* **107**, 16783–16787 (2010)
- Langmuir, I.: The constitution and fundamental properties of solids and liquids. *J. Am. Chem. Soc.* **38**(11), 2221–2295 (1916)
- Langmuir, I.: The adsorption of gases on plane surfaces of glass, mica and platinum. *J. Am. Chem. Soc.* **40**, 1361–1403 (1918)
- Lin, S.-C., Chen, Y.-C., Lin, Y.-M.: General approach for the development of high-performance liquid chromatography methods for biosurfactant analysis and purification. *J. Chromatogr. A* **825**(2), 149–159 (1998)
- Lippens, B., Linsen, B., Boer, J.: Studies on pore systems in catalysts I. The adsorption of nitrogen; apparatus and calculation. *J. Catal.* **3**, 32–37 (1964)
- Mejía, A., Requena, B., Rivera, D., Pardón, M., Rais, J. Agua potable y saneamiento en América Latina y el Caribe: metas realistas y soluciones sostenibles. Caracas: CAF. <http://scioteca.caf.com/handle/123456789/499> (2012). Accessed 20 Oct 2018
- Miguel, G., Fowler, G., Sollars, C.: Pyrolysis of tire rubber: porosity and adsorption characteristics of the pyrolytic chars. *Ind. Eng. Chem.* **37**, 2430–2435 (1998)
- Minoui, S., Minai, D.: Effect of Triton X-100 on bioremediation of PAHs of medium crude oil in soil. *Bioremediation, Biodivers Bioavailab.* **3**(2), 79–83 (2009)
- Miranda, R., Segovia, C., Sosa, C.: Pirólisis de Llantas Usadas: Estudio Cinético e Influencia de Variables de Operación. *Inf. Tecnol.* **17**(2), 7–14 (2006)
- Mohan, P., Nakhla, G., Yanful, E.: Biodegradability of surfactants under aerobic, anoxic, and anaerobic conditions. *J. Environ. Eng.* **132**, 279–283 (2006)
- Niranjana, E., Raghavendra, R., Kumara, B., Sherigara, B., Jayadevappa, H.: Studies on adsorption of Triton X-100 at carbon paste and ceresin wax carbon paste electrodes and the enhancement effect in dopamine oxidation by cyclic voltammetry. *Int. J. Electrochem. Sci.* **2**, 923–934 (2007)
- Otowa, T., Tanibata, R., Itoh, M.: Production and adsorption characteristics of MAXSORB: high-surface-area activate carbon. *Gas Sep. Purif.* **7**(4), 241–245 (1993)
- Paria, S., Khilar, K.: A review on experimental studies of surfactant adsorption at the hydrophilic solid–water interface. *Adv. Colloid Interface Sci.* **110**, 75–95 (2004)
- Parra, R.: Digestión anaeróbica: mecanismos biotecnológicos en el tratamiento de aguas residuales y su aplicación en la industria alimentaria. *Producción + Limpia.* **10**(2), 142–159 (2015)
- Passaponti, M., Rosi, L., Savastano, M., Giurlani, W., Miller, H.: Recycling of waste automobile tires: transforming char in oxygen reduction reaction catalysts for alkaline fuel cells. *J. Power Sour.* **427**, 85–90 (2019)
- Pedram, A., Yusoff, N., Udony, O., Mahat, A., Pedram, P., Babalola, A.: Integrated forward and reverse supply chain: a tire case study. *Waste Manage.* **60**, 460–470 (2017)
- Redlich, O., Peterson, D.: A useful adsorption isotherm. *J. Phys. Chem.* **63**(6), 1024–1026 (1959)
- Robson, R., Dennis, E.: The size, shape, and hydration of nonionic surfactant micelles Triton X-100. *J. Phys. Chem.* **81**(11), 1075–1078 (1997)
- Rofiqul, I., Haniu, M., Rafiqul, M.: Liquid fuels and chemicals from pyrolysis of motorcycle tire waste: product yields, compositions and related properties. *Fuel* **87**, 3112–3122 (2008)
- Romero, M., Rodríguez, A., Nieves, J.: Adsorption and desorption of Triton X-100 in polystyrene particles with different functionality. *J. Colloid Interface Sci.* **227**, 329–333 (2000)
- Rosen, M.: *Surfactants and Interfacial Phenomena*, 3rd edn. Wiley, New York (2004)
- Rouquerol, F., Rouquerol, J., Sing, K.: *Adsorption by Powders and Porous Solids Principles, pp. 1–6. Methodology and Applications.* Academic Press, San Diego (1999)
- Seidelt, S., Müller, M., Bockhorn, H.: Description of tire pyrolysis by thermal degradation behaviour of main components. *J. Anal. Appl. Pyrolysis.* **75**, 11–18 (2006)
- Stuart, B.: *Infrared Spectroscopy: Fundamentals and Applications.* Wiley, Hoboken (2004)
- Talu, O., Meunier, F.: Adsorption of associating molecules in micropores and application to water on carbon. *AIChE J.* **42**(3), 809–819 (1996)
- Technavio.: *Global Triton X-100 Market - Rising Prominence for Biosurfactants To Promote Growth.* Publishing Business Wire. <https://businesswire.com/news/home/20180213006228/en/Global-Triton-X-100-Market—Rising-Prominence> (2018). Accessed Sept 2018
- Teng, H., Lin, C., Hsu, L.: Production of activated carbons from pyrolysis of waste tires impregnated with potassium hydroxide. *J. Air Waste Manage. Assoc.* **50**, 1940–1946 (2000)
- Thommes, M., Kaneko, K., Neimark, A.V., Olivier, J.P., Rodriguez, F., Rouquerol, J., Sing, J.: Physisorption of gases, with special reference to the evaluation of surface area and pore size distribution (IUPAC Technical Report). *Pure Appl. Chem.* **87**, 1051–1069 (2015)
- Torrado, C., Franco, A., Fernández, C.: Development of adsorbents from used tire rubber: their use in the adsorption of organic and inorganic solutes in aqueous solution. *Fuel Sci. Technol.* **92**(2), 206–212 (2011)
- Toth, J.: State equations of the solid gas interface layer. *Acta Chem. Acad. Hung.* **69**, 311–317 (1971)
- Wang, J., Kaskel, S.: KOH activation of carbon-based materials for energy storage. *J. Mater. Chem.* **22**, 23710–23715 (2012)
- Yakout, M.: Monitoring the changes of chemical properties of rice straw-derived biochars modified by different oxidizing agents and their adsorptive performance for organics. *Bioremediat. J.* **19**, 171–182 (2015)
- Yakout, S., Nayl, A.: Removal of cationic surfactant (CTAB) from aqueous solution on to activated carbon obtained from corncob. *Carbon- Sci. Technol.* **2**, 107–116 (2009)
- Zahoor, M.: Separation of surfactants from water by granular activated carbon/ultrafiltration hybrid process. *Desalin. Water Treat.* **57**(5), 1988–1994 (2016)
- Zeng, G., Zhong, H., Yuan, X., Fu, M., Wang, W., Huang, G.: Codegradation with glucose of four surfactants, CTAB, Triton X-100, SDS and rhamnolipid, in liquid culture media and compost matrix. *Biodegradation* **18**, 303–310 (2007)
- Zeppieri, S., Ramírez, Y., Molina, J., Lopéz, A.: Estudio experimental de la tensión interfacial transitoria para sistemas Alcanos-Agua-Triton X-100 empleando la Técnica de la Gota Emergente. *Inf. Tecnol.* **20**(6), 125–135 (2009)

Publisher's Note Springer Nature remains neutral with regard to jurisdictional claims in published maps and institutional affiliations.